

Manifold Optimisation Assisted Gaussian Variational Approximation

Bingxin Zhou, Junbin Gao, Minh-Ngoc Tran and Richard Gerlach

Abstract—Variational approximation methods are a way to approximate the posterior in Bayesian inference especially when the dataset has a large volume or high dimension. Factor covariance structure was introduced in previous work with three restrictions to handle the problem of computational infeasibility in Gaussian approximation. However, the three strong constraints on the covariance matrix could possibly break down during the process of the structure optimization, and the identification issue could still possibly exist within the final approximation. In this paper, we consider two types of manifold parameterization, Stiefel manifold and Grassmann manifold, to address the problems. Moreover, the Riemannian stochastic gradient descent method is applied to solve the resulting optimization problem while maintaining the orthogonal factors. Results from two experiments demonstrate that our model fixes the potential issue of the previous method with comparable accuracy and competitive converge speed even in high-dimensional problems.

Index Terms—Variational Approximation; Bayesian Variational Encoder; Riemannian Manifolds; Stiefel Manifolds; Grassmann Manifolds; Riemannian Conjugate Gradient Method

I. INTRODUCTION

Variational approximation methods are an alternative way to conventional Monte Carlo algorithms for implementing Bayesian inference. The complex posterior density could be efficiently collected to a close form especially when the dataset has a large volume or high dimension. The approximations estimate the full posterior without any additional step to perform inference, and the deterministic optimization algorithms can easily assess convergence by examining the objective function value change [7].

In the context of Gaussian variational approximation, one needs to estimate the full covariance matrix for the model parameters, although most methods assume a diagonal covariance matrix for the sake of simple computation. In the case of full covariance matrix, the number of matrix elements grows quadratically in high dimension scenarios, where the computational cost become too expensive to solve the problems. Alternatively, parameterizing the covariance matrix is required to build a faster optimization procedure. There exist various strategies in literature for parameterizing the covariance matrices in Gaussian variational approximation, while many of them require special assumptions or restrictions. Researchers [8], [13] created importance-weighted auto-

encoders by applying boosting method. The approximated posterior is updated recursively to add the correlations between factors and describe complex mixture distributions. The other method was proposed by Ong et al. [15] to factorize the covariance structure to a generalized form. Stochastic gradient method is applied to update the estimation of the marginal likelihood. In their work, no specific conjugate structure is pre-request for the prior density or a factorizing likelihood. Later, they [16] pointed out that the number of parameters could be extremely high and the previous methods would have a slow convergence speed. To deal with the problem, they proposed a likelihood-free inference with synthetic likelihood surface to include a shrinkage factor. These methods simplify the generalization process to other types of distribution. Meanwhile, the computing speed is significantly boosted especially in high-dimensional scenarios. However, the factors in variational Bayes with synthetic likelihood (VBSL) algorithms of [15], [16] follow stringent restrictions for solving the identification issue. These restrictions could fail to stick to during the process of stochastic gradient updating. At least, there is no guarantee of satisfying the restrictions.

In recent years, the nonlinear optimization methods on manifolds have caught great attention, where the additional constraints such as rank and orthogonality could easily be handled for an optimization problem [2]. There have been great development and applications of manifold optimization methods in machine learning [10], [18]. Both Stiefel manifold and Grassmann manifold have played key roles in learning tasks. For example, Dong et al. [5] used Grassmann manifolds to cluster graphs by combining multi-layer results to a low dimensional representation, and Farseev et al. [6] further improved the clustering method on complementary data sources to project group knowledge on the Grassmann manifold and detect user community. Except for this, the Grassmann manifold optimization is often used for matrix completion tasks. A sparse matrix can be reconstructed by a representative matrix of minimum rank that matches the known entries with affine constraints [11], [14]. On the other hand, Stiefel manifold methods are widely used in pattern recognition [3], [26], dimension reduction [22], [23] and other fields.

When optimizing a nonlinear problems with structural constraints, it could be particularly useful to formulate them on a specific type of manifold and employ a Riemannian optimization algorithm. Currently, the approach is mostly applied for solving low-rank problems. For example, Vandereycken and Vandewalle [25] approximated low-rank matrices with a few sub-samples of themselves with low requirements of

This project is supported by the Grant from Pilot Research Scheme provided by the University of Sydney Business School.

Bingxin Zhou, Junbin Gao, Minh-Ngoc Tran and Richard Gerlach all are with the Discipline of Business Analytics, The University of Sydney Business School, The University of Sydney, NSW 2006, Australia. E-mail: bzho3923@uni.sydney.edu.au, {junbin.gao, minh-ngoc.tran, richard.gerlach}@sydney.edu.au

memory. Sato and Iwai [21] pushed the accuracy of singular value decomposition algorithm with Newton's method on the Riemannian optimization process. Zhou et al. [28] developed a rank-constrained optimization method. The lower the rank of the objective matrix, the lower computational cost of the algorithm.

In this study, we aim to reform the original VBSL method of [15] so that the constraints could be fully maintained in the process of updating the model parameters. The main challenge to be addressed come from two perspectives. Firstly, the matrix B from the factor parameterization is required to be full rank, which would probably break down when updating under the current algorithm. Secondly, given the restriction conditions under reparameterization, the domain of the new marginal likelihood function has specific structures, i.e., naturally defined on a manifold. In this case, the classic update rules based on the Euclidean gradient become invalid.

We propose a manifold assisted optimization method, termed Man-VBSL, to address the above issues and generate more stable approximation results. We propose two manifold constraints, i.e., Stiefel and Grassmann manifolds respectively, to reparameterize the factor covariance. As a result of the modification, the strong constraints of the full-ranked factor matrix is guaranteed along the updating process. For the second issue, we apply the Riemannian stochastic gradient descent (RGD) method to optimize the parameters. Four types of gradient descent methods are used to update the factors while matching the requirements of the constraint manifold structure.

The next section reviews the related concepts and methods, including VBSL algorithm of [15], the Stiefel and Grassmann manifold and their RGD methods. Section III shows the details of the stochastic gradient descent algorithm for the optimization problem based on the developed reparameterization trick. Section IV provides empirical evidence on the advantages of the proposed method with respect to the previous VBSL method. Two real data examples are used for estimation, and the performance is evaluated on the accuracy and computational speed. Section V summarizes the work.

II. PRELIMINARY

We start with reviewing the stochastic gradient variational Bayes.

A. Gaussian Variational Approximation

Our work is primarily related to the stochastic gradient variational Bayes for Gaussian variational approximation. We use $q_\lambda(\theta)$ for a member of the approximating family where λ denotes the variational parameters that determine the mean and covariance matrix. The target of the variational approximation methods is to maximize the variational lower bound $\mathcal{L}(\lambda)$, i.e.

$$\begin{aligned} \mathcal{L}(\lambda) &= \int \log \frac{p(\theta)p(y|\theta)}{q_\lambda(\theta)} q_\lambda(\theta) d\theta \\ &= \mathbb{E}_q[\log h(\theta) - \log q_\lambda(\theta)], \end{aligned} \quad (1)$$

where $h(\theta) = p(\theta)p(y|\theta)$.

The stochastic gradient methods optimize the objective function by recursively repeating

$$\lambda^{(t+1)} = \lambda^{(t)} + \alpha_t \nabla_\lambda \widehat{\mathcal{L}}(\lambda^{(t)}),$$

until converge, where α_t is the learning rate of the gradient, and t indicates the step of the iteration.

In the work of [15], the factor parameterization of the variational distribution assumes that $q_\lambda(\theta) = \mathcal{N}(\mu, \Sigma)$ with the mean vector μ and the covariance matrix

$$\Sigma = BB^T + D_2^2, \quad (2)$$

where B is an $m \times p$ full rank matrix with $p \leq m$ and D_2 is a diagonal matrix with diagonal elements in vector $d_2 = (d_{21}, \dots, d_{2m})^T$.

For the given variational Gaussian and the covariance $\Sigma = BB^T + D_2^2$, the second term in (1) can easily be calculated as

$$\mathbb{E}_q[\log q_\lambda(\theta)] = -\frac{1}{2} \log |BB^T + D_2^2| - \frac{m}{2} (\log(2\pi) + 1).$$

While the target is to find the argument λ that maximizes the lower bound, the constant terms could be neglected. As a result, the objective log likelihood function could be rearranged as

$$\mathcal{L}(\lambda) = \mathbb{E}_q[\log h(\theta)] + \frac{1}{2} \log |BB^T + D_2^2|.$$

The chosen variational Gaussian with the given factorizing covariance allows applying the so-called the reparameterization trick of [12] and [17] to obtain efficient gradient estimates for stochastic gradient variational inference. Let $f(z, \epsilon)$ as the density of $\mathcal{N}(\mathbf{0}, I)$ in the generative representation of $q_\lambda(\theta)$, then $\theta = \mu + Bz + d_2 \circ \epsilon$, and

$$\mathcal{L}(\lambda) = \mathbb{E}_f[\log h(\mu + Bz + d_2 \circ \epsilon)] + \frac{1}{2} \log |BB^T + D_2^2|.$$

The re-formulation step provides an explicit explanation by a small number of latent variables with the additional independent error term $d_2 \circ \epsilon$.

The identification issue is a potential problem of the method. Consider any orthogonal matrix Q of size $p \times p$, it is easy to see that

$$|BQ(BQ)^T + D_2^2| = |BB^T + D_2^2|$$

and

$$\mathbb{E}_f[\log h(\mu + B(Qz) + d_2 \circ \epsilon)] = \mathbb{E}_f[\log h(\mu + Bz + d_2 \circ \epsilon)]$$

as Qz is a standard Gaussian distribution as well.

To resolve the threat, in both [15] and [24], more restrictions are suggested on the factor matrix B . Specifically, B is required to be a lower triangular matrix with positive diagonal elements, and the column rank has to be full. However, the currently developed optimization algorithms may not guarantee that at each iteration step the updated factor matrix B is of full rank. One example is the stochastic gradient descent in [15]. Considering the simplest situation with a static learning rate $\alpha = 0.01$. Suppose we have $B^{(t)} = \begin{bmatrix} 1 & 0 \\ 2 & -1 \end{bmatrix}$. When the

gradient $\frac{\partial \mathcal{L}(B)}{\partial B} = \begin{bmatrix} 2 & 0 \\ 50 & 100 \end{bmatrix}$, the updated $B^{(t+1)}$ after one step of gradient compute becomes $\begin{bmatrix} 1.02 & 0 \\ 2.5 & 0 \end{bmatrix}$.

The rank of the matrix decreases from 2 to 1. While the result $B^{(t+1)}$ is no longer full rank, the update rule is invalid.

We propose Man-VBSL as a manifold implementation to guarantee an identified solution while getting rid of stringent restrictions of the factor structure. Two efficient reparameterization methods are introduced with Stiefel manifold constraint and Grassmann manifold constraint, respectively. The required result could either be provided as a set of bases from the Stiefel manifold, or be represented as a subspace that comes from a Grassmann manifold.

B. Stiefel Manifold Constraint

Definition 1 (The Stiefel Manifold [1]). *Let $p \leq m$, the Stiefel manifold $\mathcal{S}(m, p)$ is the set of $m \times p$ -dimensional matrices consisting of orthonormal columns. That is*

$$\mathcal{S}(m, p) = \{B : B^T B = I_p\}.$$

Let $B \in \mathcal{S}(m, p)$ be any Stiefel manifold point, i.e. $B^T B = I_p$, and both D_1 and D_2 are diagonal matrices of size $p \times p$ and $m \times m$, respectively.

For the assumed variational Gaussian distribution $q_\lambda(\theta) = \mathcal{N}(\mu, \Sigma)$, we take the following reparameterization for the covariance

$$\Sigma = B D_1^2 B^T + D_2^2. \quad (3)$$

Suppose (z, ϵ) follows the standard $(p + m)$ -dimensional Gaussian distribution, then θ defined by the following transformation will follow $\mathcal{N}(\mu, \Sigma)$

$$\theta = \mu + B D_1 z + d_2 \circ \epsilon.$$

We will use f to denote the standard Gaussian distribution of (z, ϵ) .

Remark 1: In the above transformation, we introduce a scaling factor D_1 to compensate the loss of scale due to the orthogonality requirement. Also D_1 can be used to avoid the identification issue of B .

The next step, similar as [12] and [17], is to update the log-likelihood function. Applying the new reparameterization trick (3) gives the new form of the lower bound of the expectation with respect to $q_\lambda(\theta)$

$$\begin{aligned} \mathcal{L}(\lambda) = & \mathbb{E}_f [\log h(\mu + B D_1 z + d_2 \circ \epsilon)] \\ & + \frac{1}{2} \log |B D_1^2 B^T + D_2^2| = \mathcal{L}_1(\lambda) + \mathcal{L}_2(\lambda), \end{aligned} \quad (4)$$

where all the constants that are irrelevant to parameter $\lambda = \{\mu, B, D_1, D_2\}$ have been ignored and the expectation \mathbb{E}_f is with respect to the standard Gaussian distribution $f(z, \epsilon) = \mathcal{N}(0, I)$.

The Stiefel manifold constraint promises the rank of the factor matrix B to be full on the column. It defines B as an orthogonal matrix. Consequently, the gradient estimates for the stochastic gradient variational inference should be conducted based on its manifold geometry.

C. Grassmann Manifold Constraint

Definition 2 (The Grassmann Manifold [1]). *The Grassmannian manifold, denoted by $\mathcal{G}(m, p)$, consists of all the p -dimensional subspaces in \mathbb{R}^m ($p \leq m$). Any Grassmannian point on $\mathcal{G}(m, p)$ can be represented by an $m \times p$ matrix B with orthonormal columns, that is, $B^T B = I_p$.*

A Grassmannian point on $\mathcal{G}(m, p)$ is indeed an equivalent class over Stiefel manifold $\mathcal{S}(m, p)$, i.e., for a representative $B \in \mathcal{S}(m, p)$, its equivalent class

$$[B] = \{BQ : B \in \mathcal{S}(m, p) \text{ and } Q \in \mathcal{O}(p)\}$$

where $\mathcal{O}(p)$ is the orthogonal group of order p [1].

The Grassmannian point is the subspace spanned by the columns of the factor B , which is a representative of the Grassmann point. The constraints of the Grassmann point B is similar to Stiefel manifold points, that each point on the subspace could be represented by an orthonormal matrix under the meaning of equivalent class.

Now we consider the following reparameterization for the variational Gaussian distribution $q_\lambda(\theta) = \mathcal{N}(\mu, \Sigma)$ with the following parameterized covariance

$$\Sigma = D_1 B B^T D_1 + D_2^2. \quad (5)$$

where D_1 is a diagonal of size $m \times m$.

Remark 2: Compared to the parameterization (2), we have introduced a scaling factor D_1 due to Grassmann orthogonality requirement. However we can remove D_1 by taking the same parameterization (2) while B is regarded as a Grassmann representative.

The parameterization (5) prompts the following variable transformation from the standard Gaussian variable (z, ϵ) to θ as

$$\theta = \mu + D_1 B z + d_2 \circ \epsilon.$$

Under the parameterization (5), the lower bound to the log likelihood becomes

$$\begin{aligned} \mathcal{L}(\lambda) = & \mathbb{E}_f [\log h(\mu + D_1 B z + d_2 \circ \epsilon)] \\ & + \frac{1}{2} \log |D_1 B B^T D_1 + D_2^2| = \mathcal{L}_1(\lambda) + \mathcal{L}_2(\lambda). \end{aligned} \quad (6)$$

As mentioned in Remark 2, if we take $D_1 = I$ without considering scaling issue, then the objective (6) becomes (1).

$$\begin{aligned} \mathcal{L}(\lambda) = & \mathbb{E}_f [\log h(\mu + B z + d \circ \epsilon)] \\ & + \frac{1}{2} \log |B B^T + D^2| = \mathcal{L}_1(\lambda) + \mathcal{L}_2(\lambda), \end{aligned} \quad (7)$$

where B is a Grassmannian point. We have noted in the experiments that the elimination of D_1 helps stabilize the result from swinging between the maxima.

III. RIEMANNIAN STOCHASTIC GRADIENT DESCENT

After the reformulating step, the objective function (4) and (6) (or (7)) with respect to the parameter B becomes an optimization problem over Stiefel manifold and Grassmann manifold, respectively. As the tradition, to work the optimal solution λ , we will minimize the negative objective $-\mathcal{L}(\lambda)$ by using the gradient descent method. However, the traditional

GD update method is based on the Euclidean distance neglecting the manifold constraints, and thus fail to converge properly in solving (4) and (6) (or (7)).

We will adopt the Riemannian Gradient Descent (RGD) algorithm to optimize (4) and (6) (or (7)). On Riemannian manifolds, the line search gradient descent algorithm has been fully described in [1]. Recently authors in [19] discussed the accelerated optimization techniques to deliver efficient and constrained-aware SGD methods, i.e., the momentum SGD (Stochastic Gradient Descent) algorithm under the framework of optimization over manifolds.

The RGD algorithm defines a descent search path over tangent space at the current point on the manifold according to the so-called Riemannian gradient of the objective function. The parameters are then updated along the Riemannian gradient in the tangent space and then a retraction step is taken to update the solution on the manifold. In a nutshell, RGD algorithm relies on both the Riemannian gradient and the retraction operator from the tangent space to the manifold.

However calculating Riemannian gradient of the objective function depends on the manifold geometry. For those manifolds that can be embedded in the ambient Euclidean space, the Riemannian gradient can be calculated by the projection from the Euclidean gradient in the ambient space of the manifold onto the tangent space at the point B of a real-valued function $\mathcal{L}(B)$ defined on the manifold. That is,

$$\text{grad}\mathcal{L}(B) = \pi_B \left(\frac{\partial\mathcal{L}(B)}{\partial B} \right). \quad (8)$$

However how to implement the projection operator π_B depends on manifolds. In this paper, we are only interested in both Stiefel and Grassmann manifolds. There exist explicit projection mapping formula for the two manifolds, as summarized in Table I. Once we have found out the Riemannian gradient, the RGD step can be defined as

$$B^{(t+1)} = r_{B^{(t)}}(-\eta \text{grad}\mathcal{L}(B)|_{B^{(t)}}), \quad (9)$$

where $r_B(\cdot)$ is the so-called retraction operator which pull back the point on tangent space back to the manifold [1]. For both Stiefel and Grassmann manifolds, the retraction operator are computable, see Table I.

A. Euclidean Gradient of the Log Likelihood Function

To successfully implement the RGD method, the partial derivative of the objective function with respect to each parameter should be calculated. We consider the cases of Stiefel and Grassmann manifold separately

1) *The Stiefel Manifold Constraint:* We start with the objective function (4) in the case of Stiefel constraint. For the first term \mathcal{L}_1 in (4), it is easy to check that

$$\frac{\partial\mathcal{L}_1}{\partial\mu} = \mathbb{E}_f[\nabla_\theta \log h(\mu + BD_1z + d_2 \circ \epsilon)]; \quad (10)$$

$$\frac{\partial\mathcal{L}_1}{\partial B} = \mathbb{E}_f[\nabla_\theta \log h(\mu + BD_1z + d_2 \circ \epsilon)(z \circ d_1)^T]; \quad (11)$$

$$\frac{\partial\mathcal{L}_1}{\partial d_1} = \mathbb{E}_f[(B^T \nabla_\theta \log h(\mu + BD_1z + d_2 \circ \epsilon)) \circ z]; \quad (12)$$

$$\frac{\partial\mathcal{L}_1}{\partial d_2} = \mathbb{E}_f[\text{diag}(\nabla_\theta \log h(\mu + BD_1z + d_2 \circ \epsilon)\epsilon^T)], \quad (13)$$

where $\nabla_\theta \log h(\mu + BD_1z + d_2 \circ \epsilon) = \nabla_\theta \log h(\theta)$ which is easy to calculate.

Now we consider the second term \mathcal{L}_2 . It could be found that

$$\frac{\partial\mathcal{L}_2}{\partial B} = (BD_1^2B^T + D_2^2)^{-1}BD_1^2; \quad (14)$$

$$\frac{\partial\mathcal{L}_2}{\partial d_1} = \text{diag}(B^T(BD_1^2B^T + D_2^2)^{-1}B) \circ d_1; \quad (15)$$

$$\frac{\partial\mathcal{L}_2}{\partial d_2} = \text{diag}((BD_1^2B^T + D_2^2)^{-1}) \circ d_2. \quad (16)$$

When facing the high-dimensional problems, the computational speed and the stability on the inverse product could be a problem. Alternatively, we use the following formula for fast computation:

$$\begin{aligned} & (BD_1^2B^T + D_2^2)^{-1} \\ &= D_2^{-2} - D_2^{-2}BD_1(I + D_1B^TD_2^{-2}BD_1)^{-1}D_1B^TD_2^{-2}, \end{aligned}$$

where we have convert the inverse of an $m \times m$ matrix to an inverse of a $p \times p$ matrix.

2) *The Grassmann Manifold Constraint:* The calculation for (6) with the Grassmann manifold constraint is similar. For the first term \mathcal{L}_1 , the derivative for each parameter is:

$$\frac{\partial\mathcal{L}_1}{\partial\mu} = \mathbb{E}_f[\nabla_\theta \log h(\mu + D_1Bz + d_2 \circ \epsilon)]; \quad (17)$$

$$\frac{\partial\mathcal{L}_1}{\partial B} = \mathbb{E}_f[(\nabla_\theta \log h(\mu + D_1Bz + d_2 \circ \epsilon)) \circ d_1]z^T; \quad (18)$$

$$\frac{\partial\mathcal{L}_1}{\partial d_1} = \mathbb{E}_f[(\nabla_\theta \log h(\mu + D_1Bz + d_2 \circ \epsilon)) \circ Bz]; \quad (19)$$

$$\frac{\partial\mathcal{L}_1}{\partial d_2} = \mathbb{E}_f[\nabla_\theta \log h(\mu + D_1Bz + d_2 \circ \epsilon)\epsilon^T]. \quad (20)$$

Similarly, the derivatives on the second term of \mathcal{L}_2 are calculated as

$$\frac{\partial\mathcal{L}_2}{\partial B} = D_1(D_1BB^TD_1 + D_2^2)^{-1}D_1B; \quad (21)$$

$$\frac{\partial\mathcal{L}_2}{\partial d_1} = \frac{1}{2}\text{diag}((D_1BB^TD_1 + D_2^2)^{-1}D_1BB^T)$$

$$+ \frac{1}{2}\text{diag}(BB^TD_1(D_1BB^TD_1 + D_2^2)^{-1})$$

$$= \text{diag}((D_1BB^TD_1 + D_2^2)^{-1}D_1BB^T); \quad (22)$$

$$\frac{\partial\mathcal{L}_2}{\partial d_2} = \text{diag}((D_1BB^TD_1 + D_2^2)^{-1}) \circ d_2. \quad (23)$$

To speed up the calculation progress while stabilizing the result, the following formula is applied in the algorithm:

$$\begin{aligned} & (D_1BB^TD_1 + D_2^2)^{-1} \\ &= D_2^{-2} - D_2^{-2}D_1B(I + B^TD_1D_2^{-2}D_1B)^{-1}B^TD_1D_2^{-2}. \end{aligned}$$

B. Adaptive Step Sizes for Stochastic Gradient Descents

Consider parameter $\lambda = \{\mu, B, D_1, D_2\}$. μ, D_1, D_2 are unconstrained parameters, and the classical ADADELTA updating rules can be applied on them. ADADELTA updating rules have been proved to be efficient in speeding up stochastic gradient descent (SGD) algorithm. The detailed discussion of the updating rules could be found in Section 4 of [15].

TABLE I: Riemannian operations required for the RGD on Stiefel and Grassmann Manifolds: $\text{sym}(X) = \frac{1}{2}(X + X^T)$ and $\text{polar}(X) = UV^T$ if $X = U\Sigma V^T$ as its SVD.

Manifolds	Tangent Spaces	Projection $\pi_B(Z)$	Retraction $r_B(U)$	Parallel Transport $\Gamma_{B_1 \rightarrow B_2}(U)$
Stiefel $\mathcal{S}(m, p)$	$T_B\mathcal{S}(m, p) = \{U \in \mathbb{R}^{m \times p} : \text{sym}(B^T U) = 0\}$	$Z - B\text{sym}(B^T Z)$	$(B + U)(I + U^T U)^{-\frac{1}{2}}$	$\pi_{B_2}(U)$
Grassmann $\mathcal{G}(m, p)$	$T_B\mathcal{G}(m, p) = \{U \in \mathbb{R}^{m \times p} : B^T U = 0\}$	$(I - BB^T)Z$	$\text{polar}(B + U)$	$\pi_{B_2}(U)$

1) *The Constrained SGD with Momentum Rule:* For the manifold constraint variable B , we already have the basic RGD updating rule defined in (9). To speeding-up RGD for B , we will use one of recently proposed Constrained SGD with Momentum (cRGD-M) [19], which reads as

$$m^{(t+1)} = \zeta \Gamma_{B^{(t-1)} \rightarrow B^{(t)}}(m^{(t)}) + \eta \text{grad}\mathcal{L}(B)|_{B^{(t)}} \quad (24)$$

$$B^{(t+1)} = r_{B^{(t)}}(-m^{(t+1)}) \quad (25)$$

where $0 < \zeta$ is the momentum constant and $\Gamma_{B_1 \rightarrow B_2}(U)$ is the so-called Parallel Transport which transports the tangent vector U at B_1 to the one at B_2 , see [1]. For both Stiefel and Grassmann manifolds, the transportation can be implemented as the projection at B_2 , which is summarised in TABLE I.

2) *The Modified Constrained RMSProp Rule:* Recently, a new constrained RMSProp rule to ensure the constraint of $B^T B = I$ was proposed in [20]. Unfortunately the suggested RMSProp scheme in [20] is not implementable. Instead we would like to suggest the following revised RMSProp scheme

$$B^{(t+1)} = r_{B^{(t)}} \left(-\eta \pi_{B^{(t)}} \left(\frac{\nabla \mathcal{L}(B^{(t)})}{\text{sgn}(E(g_B^2)^{(t+1)}) \odot \sqrt{|E(g_B^2)^{(t+1)}| + \epsilon}} \right) \right) \quad (26)$$

where

$$E(g_B^2)^{(t+1)} = \zeta \Gamma_{B^{(t-1)} \rightarrow B^{(t)}}(E(g_B^2)^{(t)}) + (1 - \zeta) \pi_{B^{(t)}}(\nabla \mathcal{L}(B^{(t)}) \odot \nabla \mathcal{L}(B^{(t)})) \quad (27)$$

with \odot as the element-wise product of two matrices and $\nabla \mathcal{L} = \frac{\partial \mathcal{L}}{\partial B}$ as the Euclidean gradient of the objective function. We choose $\eta = 0.05, \zeta = 0.95$ and $\epsilon = 10^{-6}$ as the given constants.

Remark 3: The revised RMSProp can be regarded as the basic RGD with the constrained normalized Euclidean gradient, but it is different from the Euclidean RMSProp [9].

3) *The Simulated ADADELTA Rule:* Though, there exist two drawbacks with (26). First, We still need to provide a learning rate η . Except, as explained in ADADELTA paper [27], there is no unit match. To resolve the issues, the element-wise division are advised for the second equation. In other

words,

$$E(g_B^2)^{(t)} = \zeta \Gamma_{B^{(t-1)} \rightarrow B^{(t)}}(E(g_B^2)^{(t-1)}) + (1 - \zeta) \pi_{B^{(t)}}(\nabla \mathcal{L}(B^{(t)}) \odot \nabla \mathcal{L}(B^{(t)})) \quad (28)$$

$$\Delta B^{(t)} = \frac{\text{sgn}(E(\Delta B^2)^{(t-1)}) \odot \sqrt{|E(\Delta B^2)^{(t-1)}| + \epsilon}}{\text{sgn}(E(g^2)^{(t)}) \odot \sqrt{|E(g^2)^{(t)}| + \epsilon}} \odot \nabla \mathcal{L}(B^{(t)}) \quad (29)$$

$$E(\Delta B^2)^{(t)} = \zeta \Gamma_{B^{(t-2)} \rightarrow B^{(t-1)}}(E(\Delta B^2)^{(t-1)}) + (1 - \zeta) \pi_{B^{(t-1)}}(\Delta B^{(t)} \odot \Delta B^{(t)}) \quad (30)$$

$$B^{(t+1)} = r_{B^{(t)}}(-\pi_{B^{(t)}}(\Delta B^{(t)})) \quad (31)$$

where the learning rate is eliminated from the update rule. It is self-updated at each step by the previous performance of the gradient.

We will denote by RGD-Basic, cRGD-M, RMSProp and RGD-ADADELTA for the basic RGD, the RGD momentum rule and the simulated ADADELTA rule for convenience. The overall algorithm for the Man-VBSL is summarised in Algorithm 1.

Remark 4: Although we have proposed the modified RMSProp and ADADELTA rules for the Riemann manifold optimization and empirically the algorithm is convergent, it is worthwhile to explore a theoretical analysis on the algorithm convergence. We leave this for our future research.

IV. EXPERIMENT

In this Section, we evaluate the validity of our methods from two perspectives. First, we prove the method's ability of convergence. A standard dataset that has a fewer amount of features than samples ($m < n$) is used, where n is the number of samples in training dataset. In the second experiment, the performance of predictive inference is of interest. A high-dimensional covariance matrix is considered where the number of features is significantly larger than the amount of available samples ($m \gg n$).

The name of each method is simplified to indicate the manifold constraint and update method. Specifically, S denotes Stiefel manifold constraint, G1 represents Grassmann manifold constraint with $D_1 = I$ and G2 represents the ordinal Grassmann method. For example, the results under G2-RGD-Basic indicates we use the ordinal Grassmann manifold method with D_1 , and $B^{(t+1)}$ is updated by RGD-Basic rules.

In addition, all experiments are carried out on a laptop machine running 64-bit operating system with Inter Core i5-6600 3.3GHz CPU and 8G RAM, and are implemented in Matlab 2018a version.

Algorithm 1 Manifold Assisted Gaussian Variational Approximation Algorithm

Require: Initialize $\lambda \leftarrow (\mu^{(0)}, B^{(0)}, d_1^{(0)}, d_2^{(0)})$, $t \leftarrow 0$.

Ensure: $\lambda^* = \{\mu^*, B^*, d_1^*, d_2^*\}$ where B^* is a Stiefel or Grassmann Point, i.e., $B^{*T}B^* = I_p$.

- 1: **if** not stopping criteria **then**
 - 2: Generate/Sample $(z^{(t)}, \epsilon^{(t)}) \sim N(0, I)$;
 - 3: Estimate the Euclidean gradients at $\lambda^{(t)} = \{\mu^{(t)}, B^{(t)}, d_1^{(t)}, d_2^{(t)}\}$ according to (10) - (16) for the Stiefel Constraint, OR (17) - (23) for the Grassmann Constraint;
 - 4: Update the non-constrained parameters $\mu^{(t+1)}$, $d_1^{(t+1)}$ and $d_2^{(t+1)}$ according to the Euclidean ADADELTA rules;
 - 5: Calculate the Riemann gradient with respect to constrained parameter B according to (8);
 - 6: Prepare auxilliary variables $m^{(t+1)}$ by (24), OR $E(g_B^2)^{(t+1)}$ by (27), OR $E(g_B^2)^{(t)}$, $\Delta B^{(t)}$, $E(\Delta B^2)^{(t)}$ by (28) - (30);
 - 7: Update $B^{(t+1)}$ by (9) (RGD-Basic), OR by (25) (cRGD-M), OR by (26) (RMSProp), OR by (31) (RGD-ADADELTA);
 - 8: $t \leftarrow t + 1$
 - 9: **end if**
-

A. Convergence Analysis

In the first experiment, we use the ionosphere data from the UCI Machine Learning Repository to empirically demonstrate the convergence of the proposed methods. The logistic regression is applied to deal with the classification problem. The learning methods are expected to classify positive samples from negative ones. In consistent with the results from [15], the same operations are made on the co-variate matrix, where the dataset ends up with 351 samples and 111 independent variables.

The number of factor p should be specified before running the program. We test different values of p to investigate the effects of p on the converge speed and prediction accuracy. We consider $p = 1, p = 10$ and $p = 30$ for the G1-RMSProp method as an example, the other 11 methods have similar results so we skip them due to the space limitation. The randomness is reduced by averaging 30 independent runs.

Fig. 1 visualizes the three smoothed lines of lower bound, which represent the degree of convergence. We can observe the influence of the factor numbers from two aspects. First, the model generally have a more stable performance when selecting a higher p . The orange trace ($p = 30$) is the smoothest on the plot, following the yellow ($p = 10$) and blue ($p = 1$) line of estimation. This may reflect that the dataset does need sufficient factors to describe. In the experiment, we also note that, when the number of factor becomes larger, the random initialization has less influence on the process of the algorithm. However, a larger number of factors indeed increases the complexity of the algorithm, consequently, the

TABLE II: Average train and test error rates for the ionosphere data with $CV = 5, p = 4$

Method	Train Error	Test Error	Time
VAFC	0.0036	0.0822	23.04
S-RGD-Basic	0.0036	0.0793	55.60
S-cRGD-M	0.0043	0.0793	54.91
S-RMSProp	0.0043	0.0794	62.08
S-RGD-ADADELTA	0.0043	0.0793	67.89
G1-RGD-Basic	0.0071	0.0765	57.09
G1-cRGD-M	0.0050	0.0765	58.90
G1-RMSProp	0.0050	0.0765	60.50
G1-RGD-ADADELTA	0.0050	0.0765	65.48
G2-RGD-Basic	0.0036	0.0822	90.67
G2-cRGD-M	0.0036	0.0793	90.68
G2-RMSProp	0.0036	0.0793	95.04
G2-RGD-ADADELTA	0.0043	0.0765	92.31

running speed slows down significantly. On average for this case, it takes 5.2 seconds to finish one round of the full ionosphere dataset with 5,000 iteration at $p = 1$. When p increases to 10 and 30, 6.84 and 9.02 seconds are required, respectively.

Fig. 2 compares the estimation of lower bounds for the 12 methods with $p = 3$ factors after 5,000 iterations. Each row represents one of the three manifold methods. The four columns, from left to right, show the results of the four different updating methods. Generally, the shapes of the curve depend on the constraints. The shapes with Stiefel and G2 methods are steeper. All the eight methods updates their lower bounds quickly in the first 2,000 iterations. However, the speed and stability of convergence could be influenced by the update methods. For example, G1-RGD-Basic in the first column of the second row shrinks its lower bound slower than the other three G1 methods, where the orange line is wider and the grey line has more variants, compared to the other three plots in the second row. This example shows that the speeding-up rules do make contribution to the algorithm convergence.

The overall accuracy with five-fold cross-validation improved slightly. On average, 1 sample is misclassified during the training process, and 5-6 samples are misclassified in the test set. Except G2-RGD-Basic, all the other 11 methods have a lower test error. Moreover, none of these training error is lower than VAFC. At the same time of fixing the problem of updating, the new methods are less likely to overfit the data. However, the training speed is to some degree sacrificed during this process. Stiefel and Grassmann 1 methods are generally 1-2 times slower than VAFC. The four G2 methods spend the longest time to update. They are 3 times slower than VAFC. The G1 methods outperform Stiefel and G2 methods with the highest accuracy and a reasonable speed. Although moving on the same type of sphere, G1's overall converge speeds are significantly faster than G2 methods. The reason, as stated in Section III, is that the structure of G1 prevents the result from swinging around the optimization point.

B. Predictive Inference

In the second experiment, we consider the binary Leukemia cancer dataset with 7120 predictors. There are 38 samples in the training set and 34 samples in the test set. we are testing

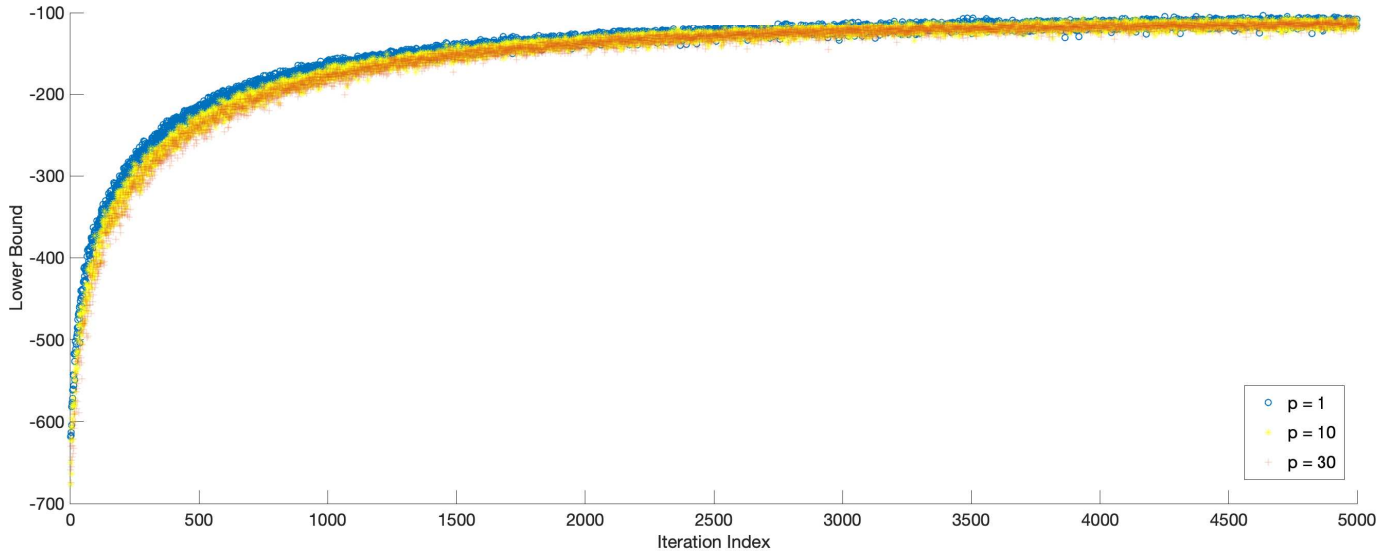


Fig. 1: Average lower bound of G1-RMSProp method with $p = 1$ (blue), 10 (yellow), 30 (red) factors. The mean value at each point is calculated by 30 independent updating results. All the 351 samples are involved in model approximation.

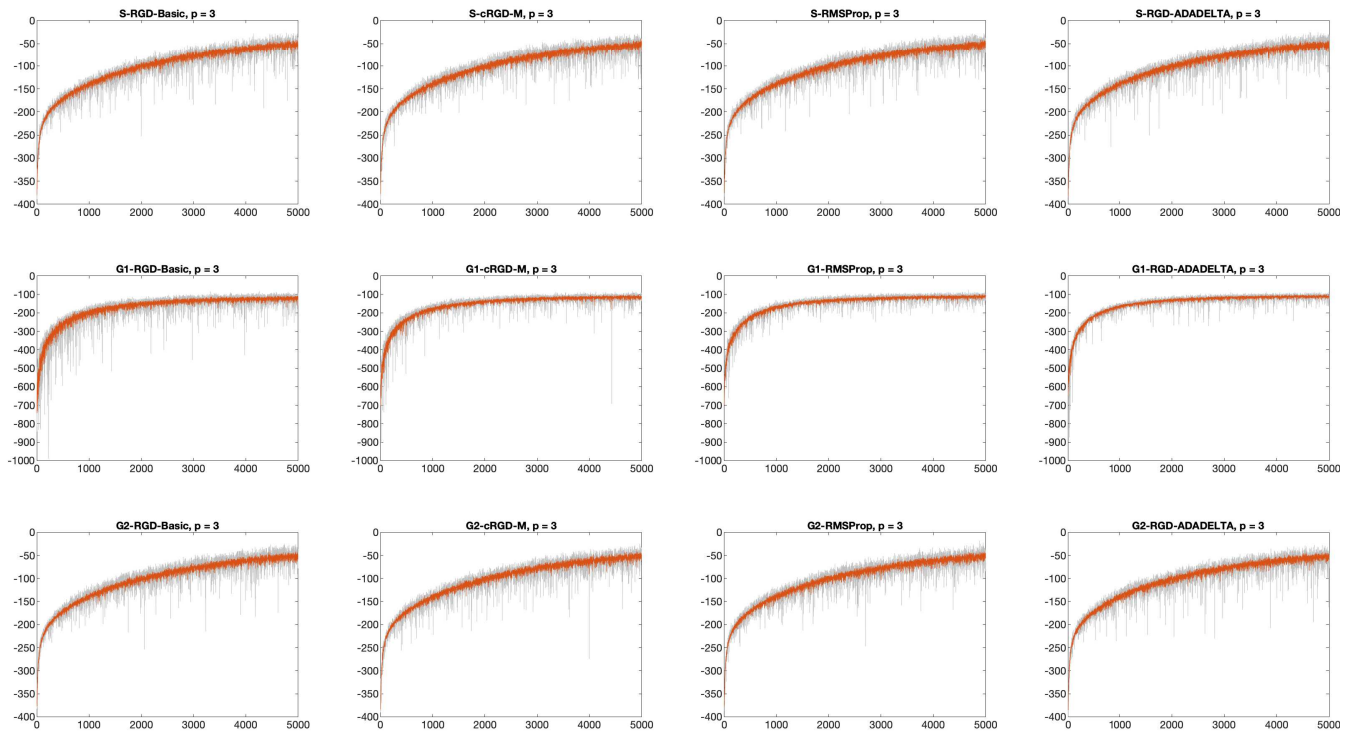


Fig. 2: Lower bound approximation of the 12 methods with $p = 3$ factors in 5000 iterations. The average convergence trace are calculated from the mean value of lower bounds for each of the methods with 10 independent rounds of updates. The results are displayed in orange. The lower bounds from the first round are drawn in grey to show the variance of one single update.

TABLE III: Average train error, test error and time for the Leukemia Cancer data with $p = 4$

Method	Training Error	Test Error	Time
VAFC	0/38	3/34	8021.71
S-RGD-Basic	0/38	2/34	10013.90
S-cRGD-M	0/38	2/34	10031.65
S-RMSProp	0/38	2/34	10011.27
S-RGD-ADELTA	0/38	2/34	10005.28
G1-RGD-Basic	0/38	2/34	6482.94
G1-cRGD-M	0/38	2/34	6438.22
G1-RMSProp	0/38	3/34	6590.98
G1-RGD-ADELTA	0/38	2/34	6202.85
G2-RGD-Basic	0/38	3/34	
G2-cRGD-M	0/38	2/34	
G2-RMSProp	0/38	2/34	5287.08
G2-RGD-ADELTA	0/38	2/34	

the method's performance of solving the classification problem in a high dimensional situation where ($m \gg n$).

In this experiment, the Horseshoe prior, as mentioned in [4], is selected to match the sparse structure. In this test we use a new stopping criterion to terminate the algorithm when the low bound increase level stays continuously at a small level of a given tolerance.

We compare the performance of the 12 methods with VAFC on both speed and accuracy in TABLE III. The first four methods with Stiefel manifold predict more accurately than VAFC with a comparable learning speed. The G1 methods have similar performance, and they also speed up the training process by 25% due to its early convergence. The performances of G2 methods are not as good as the others, because they iterate fewer times to update the coefficients so that the results could be provided after an acceptable waiting time. The updating is stopped when the relative change for the last 5 iteration is less than 0.1.

Two samples are misclassified by all the methods. Both of the samples are wrongly predicted as positive, while the true value should be negative. One of possible reasons is that the dataset is slightly unbalanced with 27 positive samples in the training set against 11 negative samples. If more samples are provided to train the model, the two samples will be more likely to be classified correctly, and our methods will perform better in that situation.

V. DISCUSSION AND CONCLUSION

This paper proposes several new manifold assisted optimization methods to resolve the identification issue existing in the Gaussian factor model in variational approximation. One of key contributions is to propose two new updating rules, i.e. Riemannian RMSProp and ADELTA, on the top of the conventional Riemannian gradient descent. All these new algorithms have been assessed by using two datasets. The experiments show the new algorithms demonstrate better performance than the benchmark VAFC in terms of model accuracy and convergence speed.

However, the overhead of optimization on manifolds is higher than its Euclidean counterpart. When a larger number of factors is needed in modeling more complicated dataset, frequent manifold retraction operation will become bottleneck for the algorithm to scale up. Although an early stopping

criterion can be adopted so that the algorithm will terminate by testing the objective function value changes, the learning process can then be accelerated at the risk of a relatively poor prediction performance.

ACKNOWLEDGEMENTS

The research project is partially supported by the Grant under the Pilot Research Scheme from the University of Sydney Business School.

REFERENCES

- [1] P.-A. Absil, R. Mahony, and R. Sepulchre. *Optimization algorithms on matrix manifolds*. Princeton University Press, 2008.
- [2] Nicolas Boumal, Bamdev Mishra, P-A Absil, and Rodolphe Sepulchre. Manopt, a matlab toolbox for optimization on manifolds. *The Journal of Machine Learning Research*, 15(1):1455–1459, 2014.
- [3] Ryan P Browne and Paul D Mcnicholas. Orthogonal stiefel manifold optimization for eigen-decomposed covariance parameter estimation in mixture models. *Statistics and Computing*, 24(2):203–210, 2014.
- [4] Carlos M Carvalho, Nicholas G Polson, and James G Scott. The horseshoe estimator for sparse signals. *Biometrika*, 97(2):465–480, 2010.
- [5] Xiaowen Dong, Pascal Frossard, Pierre Vandergheynst, and Nikolai Nefedov. Clustering on multi-layer graphs via subspace analysis on grassmann manifolds. *IEEE Transactions on signal processing*, 62(4):905–918, 2014.
- [6] Aleksandr Farseev, Ivan Samborskii, Andrey Filchenkov, and Tat-Seng Chua. Cross-domain recommendation via clustering on multi-layer graphs. In *Proceedings of the 40th International ACM SIGIR Conference on Research and Development in Information Retrieval*, pages 195–204. ACM, 2017.
- [7] Justin Grimmer. An introduction to bayesian inference via variational approximations. *Political Analysis*, 19(1):32–47, 2011.
- [8] Fangjian Guo, Xiangyu Wang, Kai Fan, Tamara Broderick, and David B Dunson. Boosting variational inference. *arXiv preprint arXiv:1611.05559*, 2016.
- [9] G. Hinton, N. Srivastava, and K. Swersky. Neural networks for machine learning: Lecture 6.1 - overview of mini-batch gradient descent. Technical report, University of Toronto, 2016.
- [10] Reshad Hosseini and Suvrit Sra. Matrix manifold optimization for gaussian mixtures. In *Advances in Neural Information Processing Systems*, pages 910–918, 2015.
- [11] Raghunandan H Keshavan, Andrea Montanari, and Sewoong Oh. Matrix completion from a few entries. *IEEE transactions on information theory*, 56(6):2980–2998, 2010.
- [12] D. P. Kingma and M. Welling. Auto-encoding variational bayes. In *Proceedings of International Conference on Learning Representation (ICLR)*, 2014.
- [13] Andrew C Miller, Nicholas Foti, and Ryan P Adams. Variational boosting: Iteratively refining posterior approximations. *arXiv preprint arXiv:1611.06585*, 2016.
- [14] Thanh Ngo and Yousef Saad. Scaled gradients on grassmann manifolds for matrix completion. In *Advances in Neural Information Processing Systems*, pages 1412–1420, 2012.
- [15] Victor M.-H. Ong, David J. Nott, and Michael S. Smith. Gaussian variational approximation with a factor covariance structure. *Journal of Computational and Graphical Statistics*, to appear:arXiv:1701.03208v1, 2019.
- [16] Victor M-H Ong, David J Nott, Minh-Ngoc Tran, Scott A Sisson, and Christopher C Drovandi. Likelihood-free inference in high dimensions with synthetic likelihood. *Computational Statistics & Data Analysis*, 128:271–291, 2018.
- [17] D. J. Rezende, S. Mohamed, and D. Wierstra. Stochastic backpropagation and approximate inference in deep generative models. In *Proceedings of the 31st International Conference on Machine Learning*, 2014.
- [18] Wolfgang Ring and Benedikt Wirth. Optimization methods on riemannian manifolds and their application to shape space. *SIAM Journal on Optimization*, 22(2):596–627, 2012.
- [19] Soumava Kumar Roy and Mehrtash Harandi. Constrained stochastic gradient descent: The good practice. In *Proceedings of the International Conference on Digital Image Computing: Techniques and Applications (DICTA)*, 2017.

- [20] Soumava Kumar Roy, Zakaria Mhammedi, and Mehrtash Harandi. Geometry aware constrained optimization techniques for deep learning. In *Proceedings of Computer Vision and Pattern Recognition (CVPR)*, pages 4460–4469, 2018.
- [21] Hiroyuki Sato and Toshihiro Iwai. A riemannian optimization approach to the matrix singular value decomposition. *SIAM Journal on Optimization*, 23(1):188–212, 2013.
- [22] Anuj Srivastava and Xiuwen Liu. Tools for application-driven linear dimension reduction. *Neurocomputing*, 67:136–160, 2005.
- [23] Taiji Suzuki and Masashi Sugiyama. Sufficient dimension reduction via squared-loss mutual information estimation. In *Proceedings of the Thirteenth International Conference on Artificial Intelligence and Statistics*, pages 804–811, 2010.
- [24] M.-N. Tran, N. Nguyen, D. Nott, and R. Kohn. Bayesian deep net GLM and GLMM. *arXiv*, page 1805.10157v1, 2018.
- [25] Bart Vandereycken and Stefan Vandewalle. A riemannian optimization approach for computing low-rank solutions of lyapunov equations. *SIAM Journal on Matrix Analysis and Applications*, 31(5):2553–2579, 2010.
- [26] John Wright, Arvind Ganesh, Shankar Rao, Yigang Peng, and Yi Ma. Robust principal component analysis: Exact recovery of corrupted low-rank matrices via convex optimization. In *Advances in neural information processing systems*, pages 2080–2088, 2009.
- [27] Matthew D. Zeiler. ADADELTA: An adaptive learning rate method. *arXiv*, 1212.5701:1–6, 2012.
- [28] Guifang Zhou, Wen Huang, Kyle A Gallivan, Paul Van Dooren, and PA Absil. Rank-constrained optimization: A riemannian manifold approach. In *In Proceeding of 23th European Symposium on Artificial Neural Networks, Computational Intelligence and Machine Learning (ESANN)*, number 1, pages 249–254, 2015.